PROCEEDINGS OF SPIE

SPIEDigitalLibrary.org/conference-proceedings-of-spie

Optimising cross-reactive plasmonic arrays for biosensing applications

Iain Christie, William Peveler, Alasdair Clark

Iain Christie, William Peveler, Alasdair W. Clark, "Optimising cross-reactive plasmonic arrays for biosensing applications," Proc. SPIE 12396, Plasmonics in Biology and Medicine XX, 1239608 (16 March 2023); doi: 10.1117/12.2649244

SPIE.

Event: SPIE BiOS, 2023, San Francisco, California, United States

Optimising Cross-Reactive Plasmonic Arrays for Biosensing Applications

Iain Christie,[a] William Peveler,[b] Alasdair W. Clark*[a]

[a] James Watt School of Engineering, Advanced Research Centre, University of Glasgow, Glasgow
[b] School of Chemistry, Joseph Black Building, University of Glasgow, Glasgow

*Corresponding author: Alasdair.clark@glasgow.ac.uk

ABSTRACT

Extraordinary optical transmission (EOT) in nanohole arrays has proven to be a useful tool for biosensing applications. The enhanced light transmission observed in these structures is due to interactions between propagating surface waves and localised resonances. In this paper we present methods to both optimise the resonance peaks of nanohole array sensors and to tune their resonance wavelength. Sensor performance is enhanced by annealing. Annealing significantly increases the grain size of the gold thin-film, reducing losses and narrowing the resonance width.[1] In addition, we show that by changing the size and arrangement of nanoholes we can control the position of their resonance peak. In doing so, we seek to improve the performance of EOT sensors for cross-reactive sensing applications.

Keywords: Plasmonics, Enhanced Optical Transmission, Nanoholes, Annealing, Biosensing

1. INTRODUCTION

Nanoholes in plasmonic materials exhibit extraordinary optical transmission (EOT). EOT results in transmission of more light through nanoholes than would be predicted by traditional aperture theory [2,3].Propagating plasmons between holes and localised plasmons within the holes combine to create this enhanced light transmission. These two modes create a concentrated electromagnetic (EM) field around the nanoholes which enhance light transmission at a wavelength defined by geometric factors.[2–5] Due to the plasmonic origin of this enhanced transmission, the transmission peak is shifted by changes in localised refractive index and as a result can be used in chemical and biological sensing applications.[6–12] In our work, we seek to use nanohole arrays as cross-reactive plasmonic sensors; a concept we have previously demonstrated with positive structures for whisky discrimination.[12]

To optimise these biosensing applications, sensor performance must be optimised. One of the metrics used to quantify sensor performance is figure of merit (FoM).

$$\mathrm{FoM}=\frac{\mathrm{Sensitivity}\ \left(\frac{\mathrm{nm}}{\mathrm{RIU}}\right)}{\mathrm{FWHM\ (nm)}} \tag{1}$$

Where RIU is refractive index units and FWHM is full width half maximum. FoM scales the sensitivity of a peak to its width and is therefore a useful metric, since the narrower the peak, the smaller the shift that can be detected.[13] As with all plasmonic structures, resonant nanoholes experience numerous sources of loss that act to dampen the resonance and increase its FWHM.[1,14] Many of these sources are intrinsic to the chosen material and are accounted for in the imaginary part of a metal's dielectric function.[14] Gold has one of the lowest intrinsic losses of commonly used plasmonic materials.[1,14] In addition to this, gold is chemically inert, biocompatible, and easy to modify with well-established thiol chemistry, making it an attractive material for plasmonic sensors.[15] One significant source of loss can be attributed to electron scattering at the grain boundaries of the gold; the fewer boundaries within the material, the less scattering takes place. Post-fabrication annealing is one way to increase the gold's grain size, reducing scattering and narrowing the resonance.[1] In addition to increasing the grain size, annealing also reduces the surface roughness of plasmonic structures, further reducing losses by diminishing the damping effects of random hotspots created by roughness, leading to a sensor with a higher

Plasmonics in Biology and Medicine XX, edited by Tuan Vo-Dinh, Ho-Pui A. Ho, Krishanu Ray
Proc. of SPIE Vol. 12396, 1239608 · © 2023 SPIE · 1605-7422 · doi: 10.1117/12.2649244

FoM.[1,13,16,17] In this paper, we show that by annealing plasmonic nanohole sensors we can maximise their FoM. We also show the control exerted over the resonance wavelength by altering their lattice pattern and hole geometry.

2. METHODS

Sensors were fabricated on borosilicate glass using electron-beam lithography (Raith EPBG 5200). Ma-N-2403 resist was spun at 3000rpm for 30s onto the substrate to create a 300nm thick resist layer. The resist was followed by 20 nm of aluminium, which acts as a conduction layer during electron-beam lithography. Once the pattern had been exposed, the aluminium was removed in TMAH solution with the resist being developed in the same solution for 5 minutes. Once the pattern was developed, a metal bilayer consisting of 2 nm titanium and 50 nm of gold was deposited. Lift off was carried out in an N-Methyl-2-pyrrolidone (NMP) based developer (Microposit Remover 1165). This process can be seen in Figure 1.

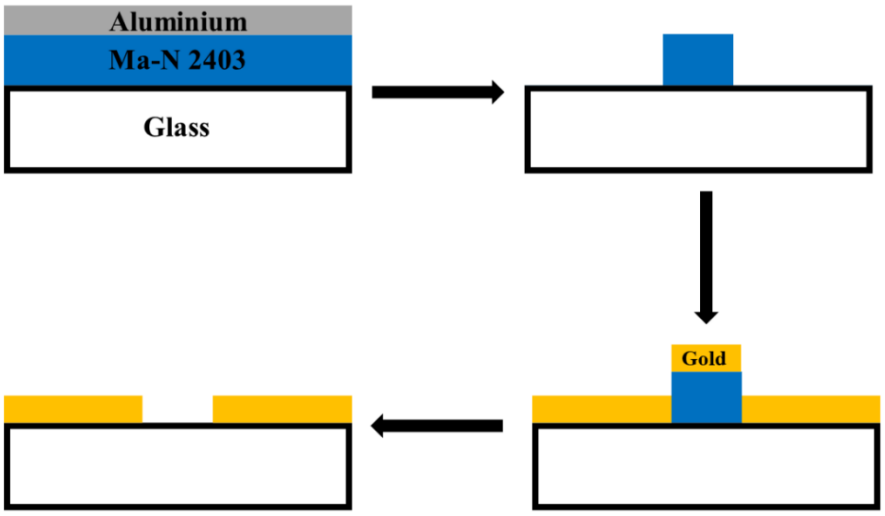

Figure 1 – A schematic depicting the fabrication process of the nanoholes using ma-N 2403 resist, electron-beam lithography, and metal evaporation.

If required, devices were then annealed using Rapid Thermal Annealing (Jipelec Jetfirst RTA) at 500˚C for 10 minutes. Spectral data was acquired using a UV/Vis spectrometer (StellarNet Blue Wave miniature spectrometer) with a 10x objective lens (Olympus Plan N) and a visible/NIR light source (StellarNet SL1 Tungsten Halogen Light Source). The spectrometer used an integration time of 350ms. Ten separate spectra were taken in rapid succession were averaged for each reading. The maxima of the spectral data was determined using a custom python script which smoothed the data and used a polynomial fit to minimise the effect of noise. Sensitivity readings are measured using water:glycerol mixtures (pure water, as well as 10% (w/w), 20% (w/w) and 30% (w/w) glycerol solutions, in water). Refractive indices of the solutions were measured using a refractometer (KERN Abbe Refractometer ORT 1RS). Five readings are taken in each solution and a best fit line was plotted through the data to get the sensitivity of each sensor in nm/RIU.

3. RESULTS AND DISCUSSION

Displayed in Figure 2 is an example of a plasmonic nanohole array before and after annealing, showing the impact annealing has on the physical and optical properties of the array. As measured by surface area, there is a shift in average grain size from 999nm^2 to 14056nm^2, a 14x increase.

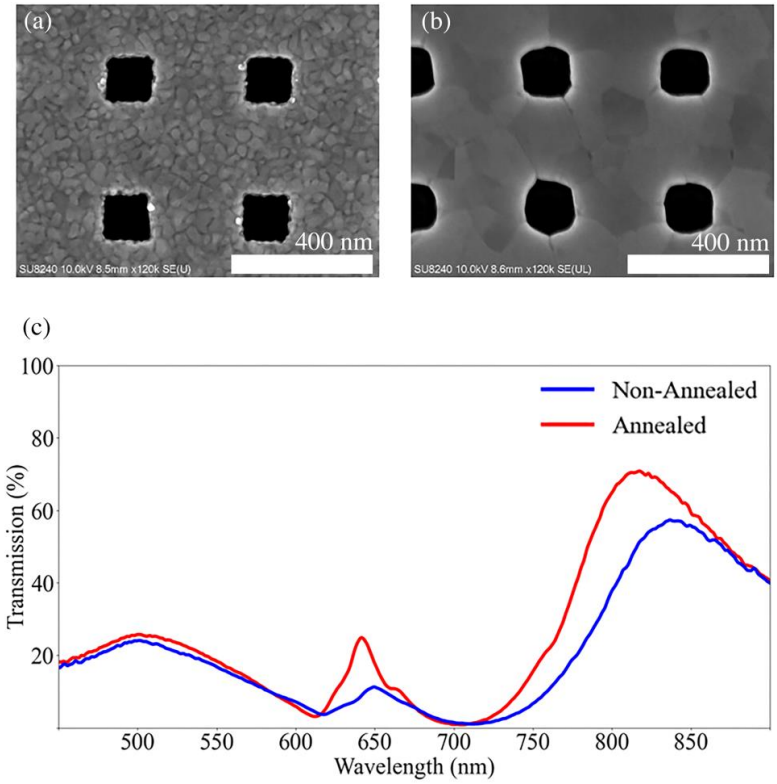

Figure 2 – Nanohole arrays before (a) and after annealing (b), along with the plasmonic spectra of the nanoholes (c).

As suggested in the literature, this annealing process blue shifts the peak while increasing height and sharpness.[1,18,19] Having a sharper peak is beneficial as it allows for more accurate tracking of small shifts in peak position created by changes in localised refractive index. To quantify this improvement, FoM is used. For the shapes displayed in Figure 1, the FoM changes from 1.31 to 2.65 after annealing. In the case of the non-annealed sensor, the range of the spectrometer means the FWHM cannot be precisely calculated as the peak is truncated. To overcome this issue, the trend of the curve is continued and is used to obtain the FWHM. Although annealing is beneficial for the plasmonic resonance it must be noted that the coalescence of the gold grains does result in a deformation of the structures with the average area of the squares increasing from 16621nm^2 to 18307nm^2. In addition to the area increasing, the standard deviation of the holes area increases with annealing, from 142nm^2 to 617nm^2. This deformation may reduce hotspots as well as increasing inhomogeneity in the array which will cause inhomogeneous broadening of the peak. These drawbacks are clearly outweighed by the benefits of annealing however, as the FoM figures suggest. As a result, all future sensors in this paper are annealed.

In addition to improving spectral quality via annealing, we also demonstrate the ability to tune the resonance peak of nanohole arrays by altering geometric parameters. Figure 3 shows how increasing the size of the nanoholes causes a red-shift in the spectra.

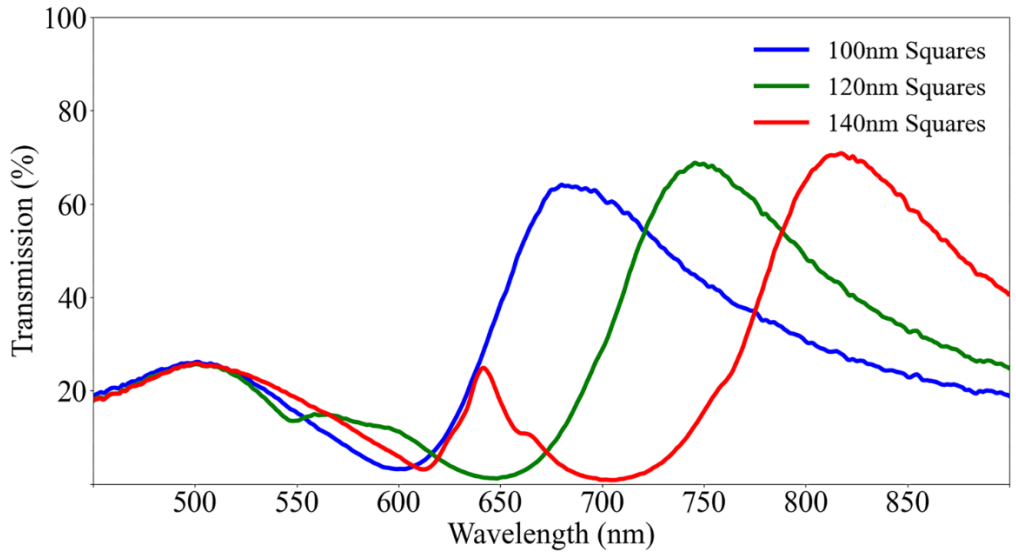

Figure 3 – The size dependence of plasmonic holes featuring 100nm (blue), 120nm (green) and 140nm (red) squares.

The periodicity of these squares is scaled with their size with each array having a periodicity 3x the size of the structures. Using a selection of glycerol solutions, the refractive index sensitivity of these sensors can be measured, as shown in Table 1. As the nanoholes increase in size, and hence increase in resonance wavelength, the sensitivity also increases. This is due to the increased sensing volume associate with higher wavelengths.[20,21]

Table 1 – The sensitivities of nanoholes of different sizes.

	100nm Squares	**120nm Squares**	**140nm Squares**
Sensitivity (nm/RIU)	210.03	233.88	270.39

In addition to changing hole size, the array spacing of the plasmonic structures also influences their resonance (Fig. 4). By changing from a square grid to a hexagonal grid, a blue shift was observed for both square and triangular nanoholes.

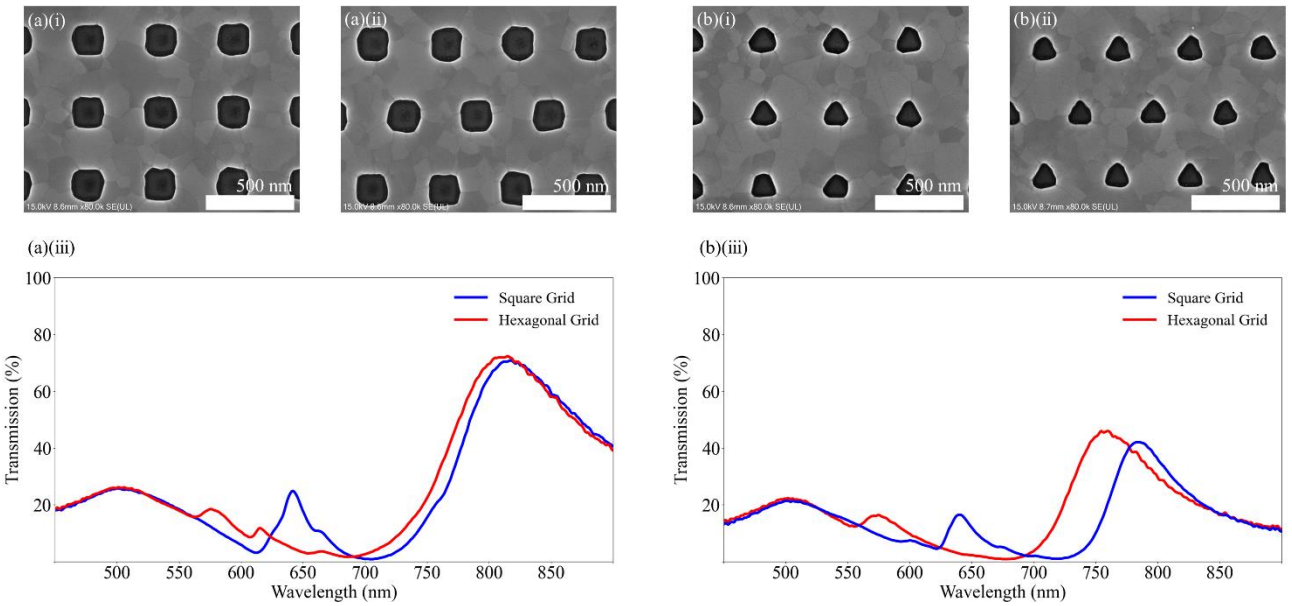

Figure 4 – Square (a) and Triangular (b) nanohole arrays and the effect of changing from a square (i) to a hexagonal (ii) lattice along with associated spectra (iii).

This blue shift can be explained using the grating coupling equations that have previously been presented in the literature.[22,23]

$$\lambda_{res} = \frac{P}{\sqrt{m^2+n^2}} \sqrt{\frac{\varepsilon_d+\varepsilon_m}{\varepsilon_d\varepsilon_m}} \tag{2}$$

$$\lambda_{res} = \frac{P}{\sqrt{\frac{4}{3}(m^2+mn+n^2)}} \sqrt{\frac{\varepsilon_d+\varepsilon_m}{\varepsilon_d\varepsilon_m}} \tag{3}$$

Where P is the periodicity of the holes, m and n are integers defining the grating order, ε_d is the dielectric constant of the media touching the metal and ε_m is the dielectric constant of the metal. Using these equations, the predicted resonance wavelength for plasmonic elements on a hexagonal grid (Eqn 3.) will always have a lower resonance wavelength compared to those on a square grid (Eqn 2.), all else being equal. Figure 3 also shows that the triangular holes have a lower maximum intensity when compared to the squares. This can be explained by the difference in fractional filling that the triangle structures will occupy (~5%) compared to the square structures (~11%).

4. CONCLUSION

In this paper we show that the resonance properties of plasmonic nanoholes can be precisely controlled by altering geometric parameters including the size of the holes and their spacing. In addition to this, we show that annealing can be highly beneficial to sensors. The reduction in losses associated with the coalescence of gold grains leads to a sharper resonance peak with a higher FoM compared to non-annealed sensors.

REFERENCES

[1] Chen, K. P., Drachev, V. P., Borneman, J. D., Kildishev, A. v. and Shalaev, V. M., "Drude relaxation rate in grained gold nanoantennas," Nano Lett **10**(3), 916–922 (2010).

[2] Genet, C. and Ebbesen, T. W., "Light in tiny holes," Nature **445**(7123), 39–46 (2007).

[3] Rodrigo, S. G., de León-Pérez, F. and Martín-Moreno, L., "Extraordinary Optical Transmission: Fundamentals and Applications," Proceedings of the IEEE **104**(12), 2288–2306 (2016).

[4] Li, Z., Clark, A. W. and Cooper, J. M., "Dual color plasmonic pixels create a polarization controlled nano color palette," ACS Nano **10**(1), 492–498 (2016).

[5] Heydari, E., Sperling, J. R., Neale, S. L. and Clark, A. W., "Plasmonic Color Filters as Dual-State Nanopixels for High-Density Microimage Encoding," Adv Funct Mater **27**(35) (2017).

[6] Im, H., Shao, H., Park, Y. il, Peterson, V. M., Castro, C. M., Weissleder, R. and Lee, H., "Label-free detection and molecular profiling of exosomes with a nano-plasmonic sensor," Nat Biotechnol **32**(5), 490–495 (2014).

[7] Li, X., Soler, M., Özdemir, C. I., Belushkin, A., Yesilköy, F. and Altug, H., "Plasmonic nanohole array biosensor for label-free and real-time analysis of live cell secretion," Lab Chip **17**(13), 2208–2217 (2017).

[8] Cetin, A. E., Etezadi, D., Galarreta, B. C., Busson, M. P., Eksioglu, Y. and Altug, H., "Plasmonic Nanohole Arrays on a Robust Hybrid Substrate for Highly Sensitive Label-Free Biosensing," ACS Photonics **2**(8), 1167–1174 (2015).

[9] Monteiro, J. P., de Oliveira, J. H., Radovanovic, E., Brolo, A. G. and Girotto, E. M., "Microfluidic Plasmonic Biosensor for Breast Cancer Antigen Detection," Plasmonics **11**(1), 45–51 (2016).

[10] Xiong, K., Emilsson, G. and Dahlin, A. B., "Biosensing using plasmonic nanohole arrays with small, homogenous and tunable aperture diameters," Analyst **141**(12), 3803–3810 (2016).

[11] Kee, J. S., Lim, S. Y., Perera, A. P., Zhang, Y. and Park, M. K., "Plasmonic nanohole arrays for monitoring growth of bacteria and antibiotic susceptibility test," Sens Actuators B Chem **182**, 576–583 (2013).

[12] Macias, G., Sperling, J. R., Peveler, W. J., Burley, G. A., Neale, S. L. and Clark, A. W., "Whisky tasting using a bimetallic nanoplasmonic tongue," Nanoscale **11**(32), 15216–15223 (2019).

[13] Offermans, P., Schaafsma, M. C., Rodriguez, S. R. K., Zhang, Y., Crego-Calama, M., Brongersma, S. H. and Gómez Rivas, J., "Universal scaling of the figure of merit of plasmonic sensors," ACS Nano **5**(6), 5151–5157 (2011).

[14] Zorić, I., Zäch, M., Kasemo, B. and Langhammer, C., "Gold, platinum, and aluminum nanodisk plasmons: Material independence, subradiance, and damping mechanisms," ACS Nano **5**(4), 2535–2546 (2011).

[15] West, P. R., Ishii, S., Naik, G. v., Emani, N. K., Shalaev, V. M. and Boltasseva, A., "Searching for better plasmonic materials," Laser Photon Rev **4**(6), 795–808 (2010).

[16] Rodríguez-Fernández, J., Funston, A. M., Pérez-Juste, J., Álvarez-Puebla, R. A., Liz-Marzán, L. M. and Mulvaney, P., "The effect of surface roughness on the plasmonic response of individual sub-micron gold spheres," Physical Chemistry Chemical Physics **11**(28), 5909 (2009).

[17] Drachev, V. P., Chettiar, U. K., Kildishev, A. v, Yuan, H.-K., Cai, W. and Shalaev, V. M., "The Ag dielectric function in plasmonic metamaterials References and links" (2008).

[18] Higashino, M., Murai, S. and Tanaka, K., "Improving the plasmonic response of silver nanoparticle arrays via atomic layer deposition coating and annealing above the melting point," Journal of Physical Chemistry C **124**(50), 27687–27693 (2020).

[19] Bosman, M., Zhang, L., Duan, H., Tan, S. F., Nijhuis, C. A., Qiu, C. W. and Yang, J. K. W., "Encapsulated annealing: Enhancing the plasmon quality factor in lithographically-defined nanostructures," Sci Rep **4** (2014).

[20] Willets, K. A. and van Duyne, R. P., "Localized surface plasmon resonance spectroscopy and sensing," Annu Rev Phys Chem **58**, 267–297 (2007).

[21] Xu, Y., Bai, P., Zhou, X., Akimov, Y., Png, C. E., Ang, L. K., Knoll, W. and Wu, L., "Optical Refractive Index Sensors with Plasmonic and Photonic Structures: Promising and Inconvenient Truth," Adv Opt Mater **7**(9) (2019).

[22] Ekşioğlu, Y., Cetin, A. E. and Petráček, J., "Optical Response of Plasmonic Nanohole Arrays: Comparison of Square and Hexagonal Lattices," Plasmonics **11**(3), 851–856 (2016).

[23] Thio, T., Ghaemi, H. F., Lezec, H. J., Wolff, P. A. and Ebbesen, T. W., "Surface-plasmon-enhanced transmission through hole arrays in Cr films" (1999).